Proceedings of the ASME 2010 3rd Joint US-European Fluids Engineering Summer Meeting and 8th International Conference on Nanochannels, Microchannels, and Minichannels
FEDSM-ICNMM2010
August 1-5, 2010, Montreal, Canada

FEDSM-ICNMM2010-31064

MAGNUS-EFFECT ROTORS FOR SOLAR CHIMNEY POWER PLANTS

Mohamed.A.Serag-Eldin
American University in Cairo
Mechanical Engineering department
AUC Avenue, New Cairo, Egypt
amrserag@aucegypt.edu

Mohammed.A.Abdul Latif
American University in Cairo
Mechanical Engineering department
AUC Avenue, New Cairo, Egypt
monofy@aucegypt.edu

ABSTRACT

The paper proposes the use of spinning and rotating cylinders to replace the axial turbines of Solar Chimney power plants. A large number of circular cylinders are placed equidistant, on a circular track concentric with the solar chimney axis. The cylinders spin around their own axis while simultaneously rotating about the chimney axis. By virtue of the Magnus effect, Lift forces arise which create force components tangential to the track in the direction of motion of the cylinders; thus mechanical work is produced. Using CFD modeling, the paper analyzes the resulting flow pattern and presents the expected performance of the hypothetical design for different geometric parameters and operating conditions. It is demonstrated that the design is indeed promising, and worthy of further investigation and development. It is also revealed that good performance of the proposed rotor is highly dependent on the proper choice of operating parameters.

keywords: Magnus effect, Solar chimney plants, solar updraft tower, turbines, aerodynamics.

INTRODUCTION

Solar chimney plants, also called solar updraft towers, [1-4], are renewable energy devices ideally suited for desert environments. They comprise three main components; namely a large solar collector, a tall stack and a circular array of horizontal axis turbines,[5-7].

The solar collector, which is similar in operation to a flat plate collector, is formed from a circular glass roof which transmits the short-wave solar radiation to the ground underneath and blocks the long wave radiation from ground to atmosphere, thus raising the temperature of the ground below by virtue of the "green-house effect". The ground, which acts as the absorber, warms the air above it. Buoyancy forces then drive the hot air up a tall chimney stack, creating a strong updraft of around 15 m/s. This updraft is employed to drive an array of turbines connected to electrical generators.

Thus the solar chimney is the effective engine of the plant which converts the solar heat energy into mechanical kinetic energy. The taller the chimney stack, the higher the pressure difference created across the wind turbine, and thus the higher the output and efficiency. The larger the collector area, the greater the air temperature-rise and the stronger the updraft. The electrical output from such a plant is approximately proportional to the cube of its size[8]. Hence by necessity commercially viable solar chimney plants are huge with capacities of the order of 200 Mw.

A proposed 200 Mw plant in Australia displayed a 1000 m high stack of 150 m diameter, with an array of 32 horizontal axis, pressure staged turbines of the axial-propeller(Kaplan) type surrounding the stack on the ground. Special nacelles and ducts surround the turbines to direct the flow and eliminate by-pass.

Among the major costs of the plants are the turbines and their ducting. Manufacturing of huge turbines, transporting them, and installing them in remote desert sites is not cheap. Moreover, they are the only large component of the plant which is not constructed locally on site. Damage to blade profiles due to sand-storms is also a likely possibility.

The objective of the present paper is to provide an alternative to the propeller-type turbines which is cost effective, may be constructed on site using local expertise, is easy to maintain and replace, as well as being resistant to the harsh desert environment. The answer lies in Manus effect rotors. To the best of the author's knowledge, the application for solar

chimney plants is new and therefore warrants investigation. This is done here with the aid of computational software.

The next section presents the proposed rotor design. The following one describes the mathematical model employed to predict the wind flow pattern and wind forces over the cylinder, from which the output work is estimated for various operating conditions and geometric parameters. Thereafter, results of the computations are displayed and discussed, and finally conclusions are presented.

PROPOSED DESIGN

Magnus effect is a well known flow phenomena which arises when a rotating cylinder spins about its axis in the face of a cross-wind. The flow pattern displays a region of increased velocity were the surface tangential velocity points in the same direction as the free stream velocity; and reduced velocity at the diametrically opposite end, where the tangential velocity opposes the free stream. Increased velocity is associated with reduced pressure and vice-versa; thus a "Lift" force is created on the cylinder, whose magnitude for idealized flow is the product of the free wind speed, air density and circulation.

Magnus effect rotors have previously been proposed for wind energy applications. The rotors were to be supported on separate carriages, Fig.1, all connected together by chains and running on a circular railway track, Fig.2. In order to keep the tangential lift force component pointing in the same direction for all cylinders, the rotational spinning speed of the individual cylinders had to be reversed once each rotation round the track. Moreover, for about half the track length the lift force displayed a small component in the tangential direction, most of the force pointing in the radial direction producing no work and increasing frictional forces with the track. Thus the design did not gain popularity.

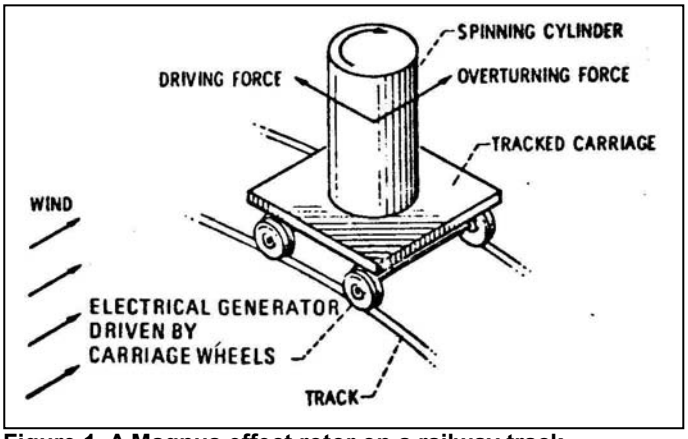

Figure 1. A Magnus effect rotor on a railway track

However, the artificial draft created by a solar updraft tower is always pointing radially inwards towards the stack, Fig.3, rather than parallel as the case for atmospheric wind. Hence the same Magnus-rotor design would always produce a tangential force pointing in same direction for all carriages while maintaining a continuous, constant direction cylinder spin. Moreover, it should be possible to align closely the lift force with the tangential direction. This is expected to render the new application much more favorable than for the atmospheric wind application.

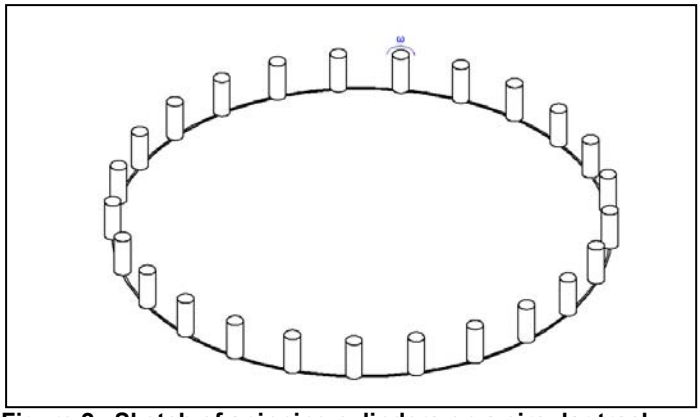

Figure 2. Sketch of spinning cylinders on a circular track

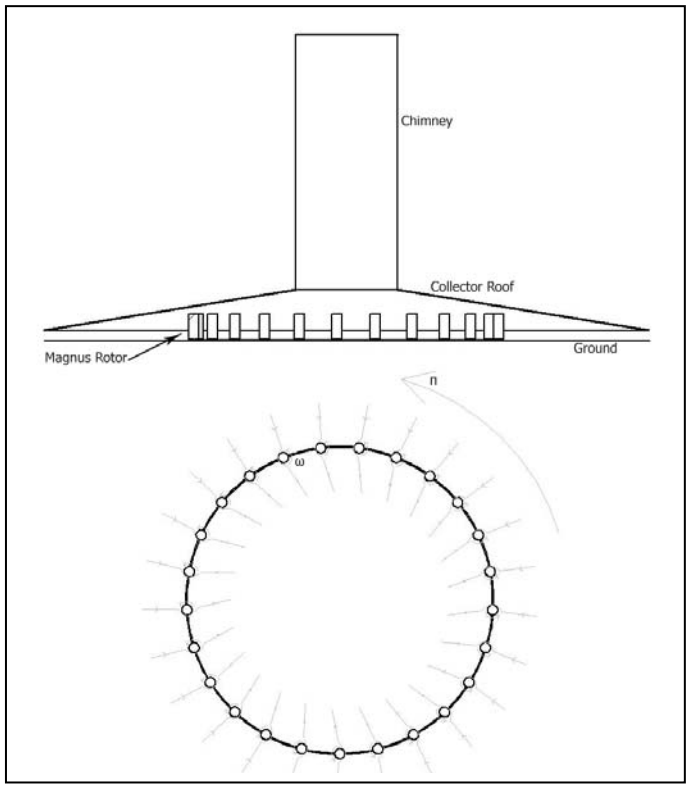

Figure 3. Installation and flow inside a Solar Chimney plant

COMPUTATIONAL MODEL

A computational model is employed to predict the flow field under various operating conditions.

Computational Domain

The computational domain is two-dimensional. It comprises an annular segment of the circle surrounding the stack axis, and subtending an included angle equal to $2\pi/n$, where n is the total number of rotating cylinders. It thus contains only a single cylinder. The radial extent of the integration domain is 20m starting from an inner radius of 240 m. The cylinders where placed at a radius of 250 m, reflecting the expected location of the rotor arrays for a 150 m diameter stack.

Turbulence Model

The high Reynold's number RNG form[10] of the k-ε turbulence model[11] is employed in the present analysis since Reynolds number of the flow is expected to be particularly high due to the large dimensions of the ducts. Enhanced near wall treatments were employed close to the wall at values of $y^+ \sim 5$.

Governing Equation

The (r,θ) cylindrical polar system of co-ordinates is employed to express the equations and describe boundary conditions; variation of dependent variables in the vertical direction was ignored since collector slope is very mild for solar updraft towers. The equations solved are those of mass conservation (continuity); momentum in radial, r and angular,θ direction; and kinetic energy of turbulence, k and its rate of dissipation ε.

Two rotations are considered here. The first of these is the rotation of the whole integration domain with a velocity Ω about the axis of the stack, while the second refers to the motion of the cylindrical surface due to the spinning about its axis with a rotational velocity ω. The first of these involves introducing appropriate acceleration terms in the momentum equations reflecting the rotating frame of reference. The second one is merely handled by moving the cylinder surface at the desired prescribed velocity relative to the rotating frame of reference.

Boundary Conditions

The integration domain is bounded by the following three types of boundaries:

i) **Inlet boundary :** This corresponds to the external radius of the integration domain. Here, a purely radial inwards flow is prescribed, yielding a radial velocity V. Turbulence intensity is prescribed to be $0.05\ V^2/2$, and its rate of dissipation is prescribed from k and the local length scale.

ii) **Exit boundary** : This corresponds to the internal radius of the integration domain. A uniform pressure boundary conditions is prescribed at this boundary, while other boundary values are prescribed default values but are not effective, because of the parabolic nature of the equations at this section(downstream effects are not transmitted upstream).

iii) **Side boundaries**: These flank the integration domain at both sides. Cyclic boundary conditions are imposed there; they imply that flow conditions entering one boundary are identical to those leaving the corresponding positions on the opposite boundary..

FLOW ANALYSIS

Three distinct motions determine the flow field in the neighborhood of the Magnus rotors, and therefore determine their performance. They are the cylinder spin about its axis, ω; the simultaneous rotational motion of the axis of the cylinders about the stack center-line, Ω; and the stack created draft of ```velocity, V. In order to facilitate the visualization of this complicated flow field, two simpler but related flows are analyzed first; they are the flow with stationary (but spinning) cylinders, and the flow with spinning and rotating cylinders in absence of the air draft.

Figure 4 displays the streamlines about a rotor whose axis is stationary(Ω=0), but otherwise spinning about its axis in the anti-clockwise direction with ω r.p.m. and subject to a 10 m/s induced draft. The induced draft direction is right-to-left and the streamlines are displayed at equal increments. High flow velocities occur where adjacent streamlines are close, and vice-versa. It is thus revealed that the flow is accelerated at the top surface of the cylinder where the surface tangential velocities is approximately pointing in the same direction as the unperturbed air draft, and decelerated at the bottom surface where it points in the opposite direction. Moreover it is noticed that at a distance of about 5 cylinder diameters, both upstream and downstream the cylinder, the flow is fairly uniform and aligned closely to the radial direction. Due to convection effects, disturbances are seen to be propagated downstream a larger distance than upstream.

Figure 5 displays the corresponding velocity vectors. These represent both the magnitude and direction of the local flow. It is seen that they are compatible with previous streamlines.

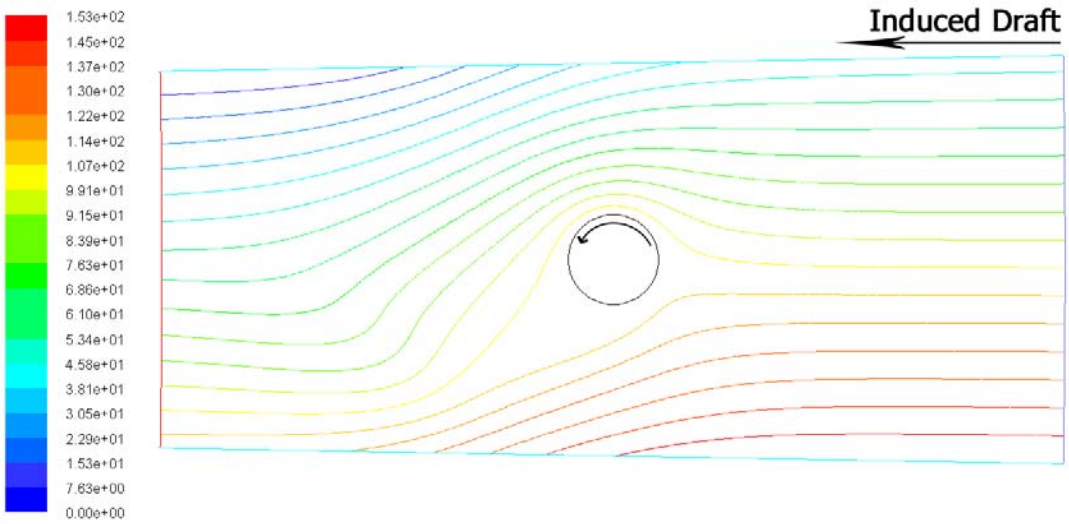

Figure 4. Streamlines about cylinder when Ω = 0.

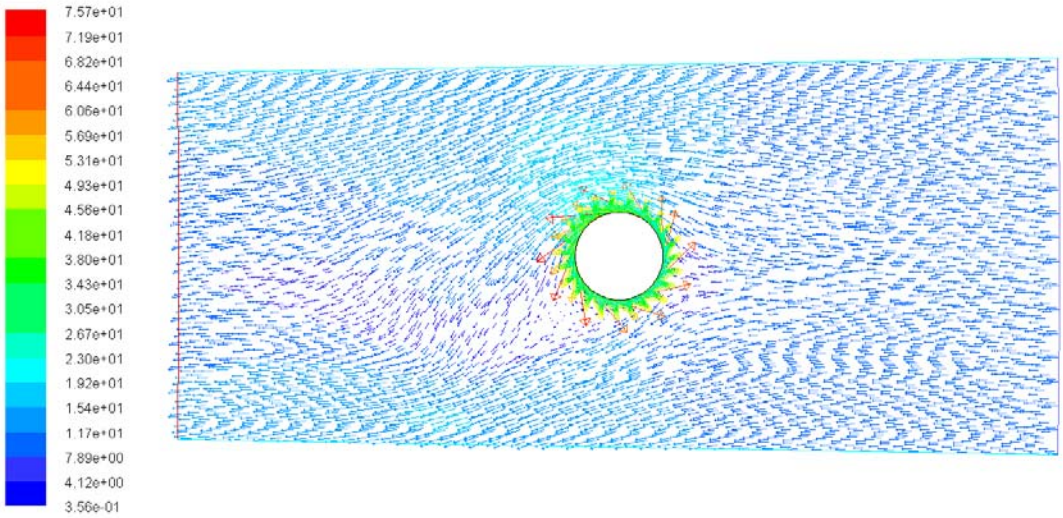

Figure 5. Velocity vectors about cylinder when Ω = 0.

Figure 6 displays the corresponding pressure contour lines. The contour lines are displayed at equal increments. The minimum value is at the top left of the cylinder, where the velocity was shown to be maximum, whereas the maximum value is at the bottom right-hand corner, where velocity was minimum. The resultant force thus points upwards, i.e. approximately perpendicular to the local radial direction. Since this case also represents conditions prevailing when starting from rest, it is gratifying to observe that the resultant force will be nearly tangential to the track and therefore producing good starting torque.

Figures(7-9) display the results corresponding to Figures(4-6), respectively, for the case when both ω and Ω rotations are present, but in absence of an induced air-draft. In order to facilitate comparison, both the plotted streamlines and velocity vectors pertain to motion relative to a reference frame moving with the cylinder axis.

Figure 7 shows that at about 5 diameters away from the cylinder the streamlines are nearly tangential to the track, since they represent the air flow with respect to the cylinder. An acceleration of flow is displayed on the left of the cylinder and a deceleration on the right. Again this is because of the alignment of the tangential surface velocity with the relative air velocity on the left side of cylinder, and opposing it on the right.

Figure 8 reveals the corresponding velocity vectors. The acceleration and deceleration of flow over both sides of cylinder is clear. Moreover a pronounced wake appears behind the cylinder.

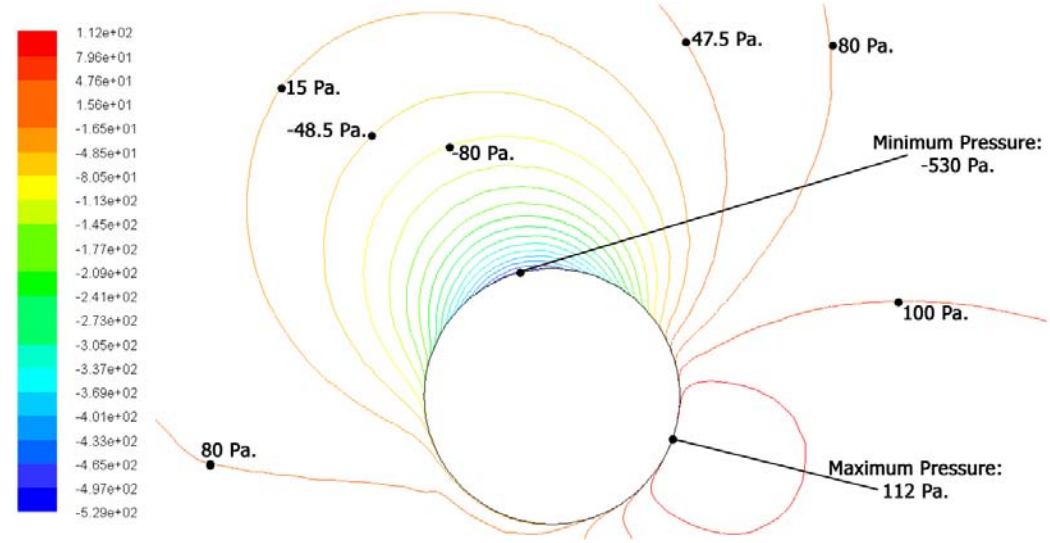

Figure 6. Static Pressure contours when Ω= 0.

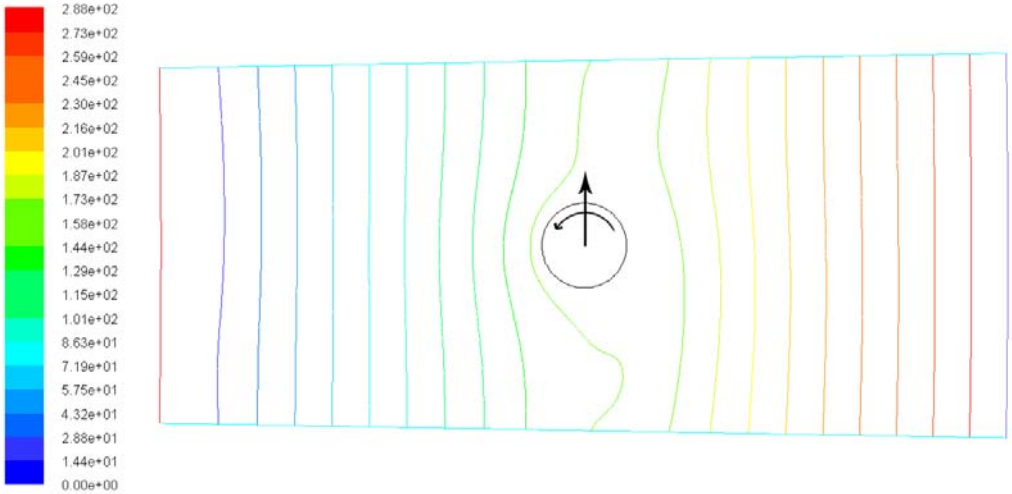

Figure 7. Air-flow Streamlines relative to cylinder when V=0.

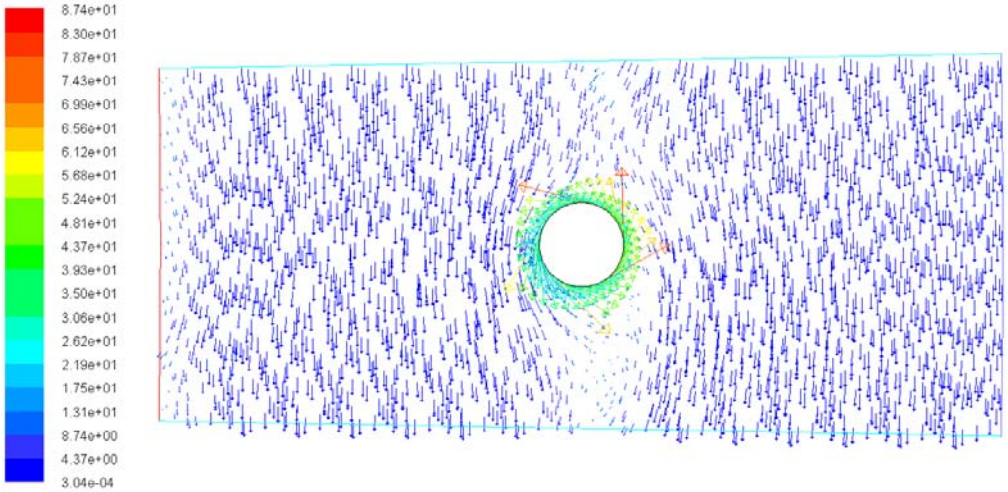

Figure 8. Velocity vectors relative to cylinder when V=0.

Figure 9 reveals the pressure contour lines surrounding the cylinder surface. It is clear that the pressure is minimum on the left side of the cylinder and maximum on the right. Thus a net lift force acting on the cylinder is created which is pointing radially inwards. This force is normal to the track and therefore to the direction of motion of the cylinders; it thus produces no work output whatsoever. It is moreover, the prime source of frictional force between cylinder and track.

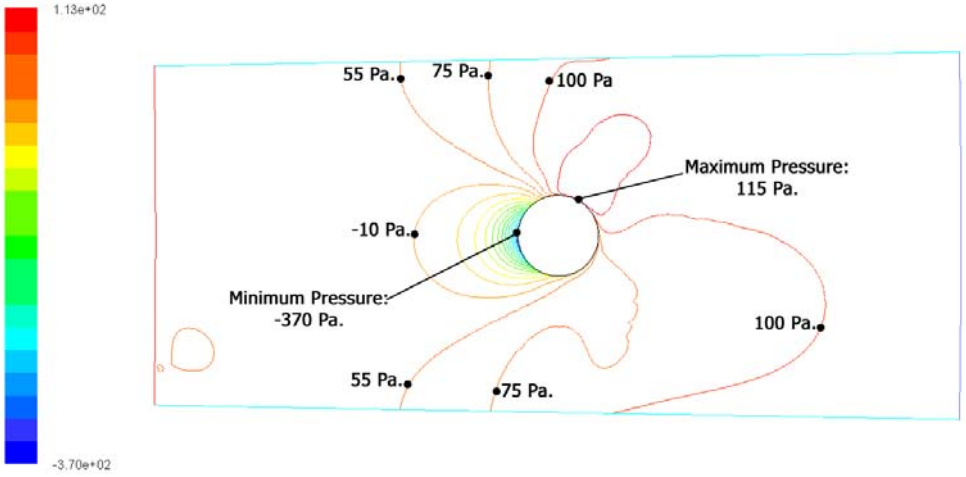

Figure 9. Static pressure contours when V=0.

The last two cases do not produce any useful work. The first because the cylinder is not moving on the track and the second because the resultant force acting on the cylinder is acting normal to the track. To get positive work output, it is necessary to allow the cylinder to move on the track, i.e. Ω≠0, in the presence of an induced draft. In this case the resulting flow will be a combination of the former two.

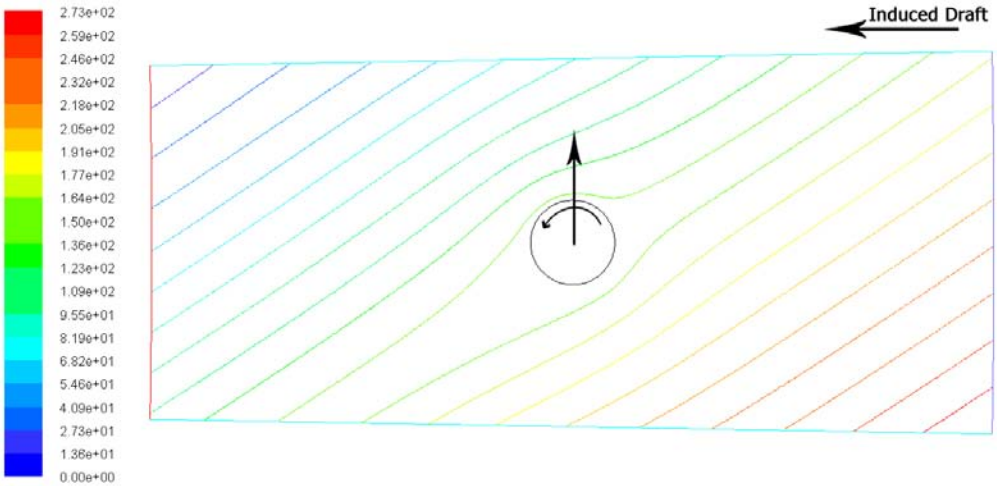

Figure 10. Streamlines relative to cylinder, ω≠0, Ω≠0, V≠0.

Figure10 displays the streamlines of the flow relative to the cylinder for the general case when all three motions are present, i.e. both spinning and rotation in presence of induced draft. The streamlines thus approach and leave making an angle with the radial direction. The angle of inclination is a function of ΩR/V.

It is apparent that an acceleration zone appears on the top left corner of the cylinder and a deceleration one almost diametrically opposite.

Figure 11 displays the corresponding vectors; a pronounced wake appears downstream the cylinder. Away from the cylinder the flow is undisturbed. Figure 12 displays the corresponding absolute velocities; it is seen that the flow enters and leaves this part of the domain almost purely radially, but is deflected near the cylinder. This deflection is what causes the forces on the cylinder.

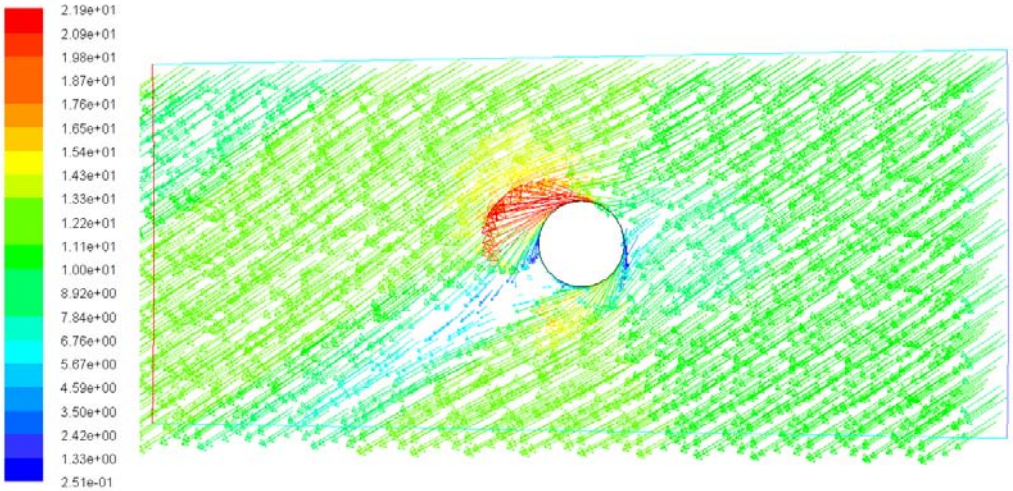

Figure 11. Relative velocities when ω≠0, Ω≠0, and V≠0.

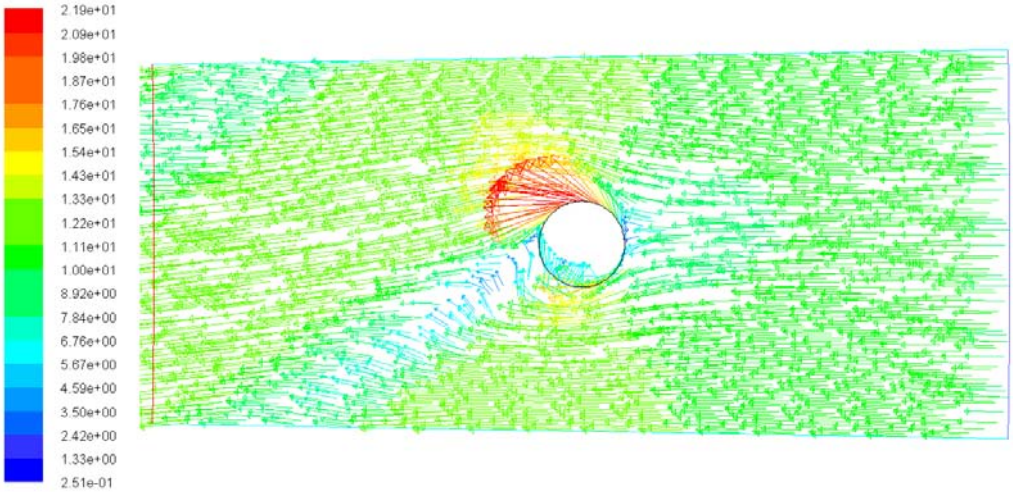

Figure 12. Absolute velocities when ω≠0, Ω≠0, and V≠0.

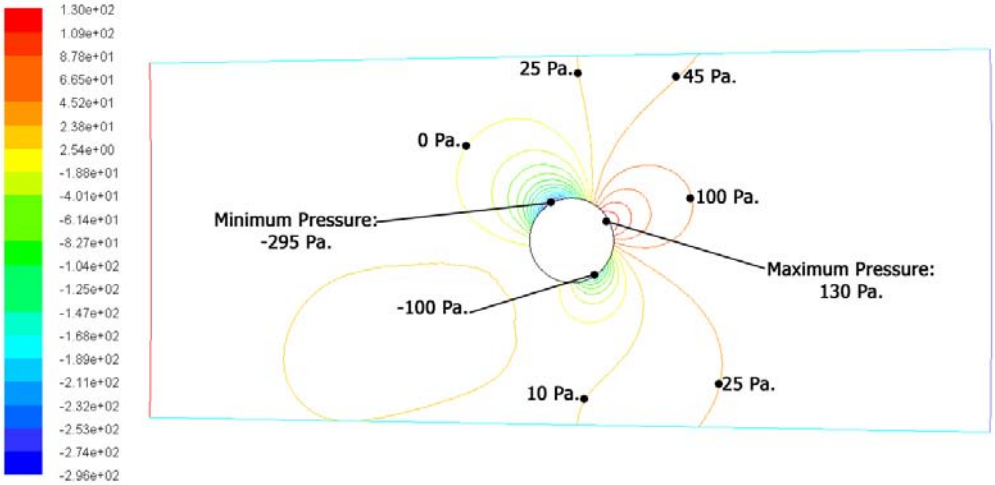

Figure 13. P contours when ω≠0, Ω≠0, and V≠0.

Figure 13 displays the pressure contour lines for this case. Minimum pressure occurs at the location of maximum velocity, whereas maximum pressure occurs close to location of the minimum velocity. The pressure distribution indicates a net lift force acting on the cylinder acting in a direction pointing inwards and upwards.

This force would display a component tangential to the track in the direction of cylinder motion, and another one normal to the track. The former produces work whereas the latter increases the friction force on the track. In addition to the lift force a drag force also exists whose component in the tangential direction usually acts in opposite direction to the motion of cylinder thus reducing net work output.

PERFORMANCE PARAMETERS

The performance of the Magnus rotor is expected to depend on ω, Ω, radius r of cylinder, radius R of track, unperturbed induced draft speed V and number of rotors n. The following dimensionless groups are formulated: the cylinder spin about its axis speed-ratio $\alpha \equiv \omega r/V$, the cylinder-axis rotation around stack speed-ratio $\beta \equiv \Omega R/V$, and the ratio of cylinder to track radii $\gamma \equiv r/R$. From these ratios other dimensionless groups may be formed. In particular the solidity ratio, S defined as $S \equiv (rn)/(\pi R) = (n\,\gamma)/\pi$.

SAMPLE CALCULATIONS

Results were obtained for many different values of ω, Ω, n, and r, and some primitive optimization was performed in order to identify the range of operation yielding highest performance. Finally, the effect of varying the absolute value of V was investigated. First explorations showed that the performance is highly sensitive to the values of the parameters selected. Indeed random values of parameters often led to the production of a net force whose track component acts in opposite direction to that of the cylinder motion, i.e. negative work.

Figure 14 displays the force vector components for 3 different ratios of γ, 5 values of α and n= 180 when the cylinders are stationary (Ω=0). Here the perpendicular lines emerging from cylinder centers represent the force vector components in the tangential and radial directions. The relative cylinder size reflects the ratio γ, whereas the segments of the circle group results of the same value of α.

The results reveal that as α increases from 0.131 to 0.656, the ratio of the tangential force component to radial component increases considerably. Since the former produces the starting torque while the latter produces friction, increase of this ratio is always welcome. Increase of the cylinder radius ratio, γ increases both the tangential and radial forces. The increase in Lift force is attributed to the increase of circulation about cylinder axis for same ω and hence same α. The increase in Drag force is attributed to the increase of surface area of cylinder with increase of r.

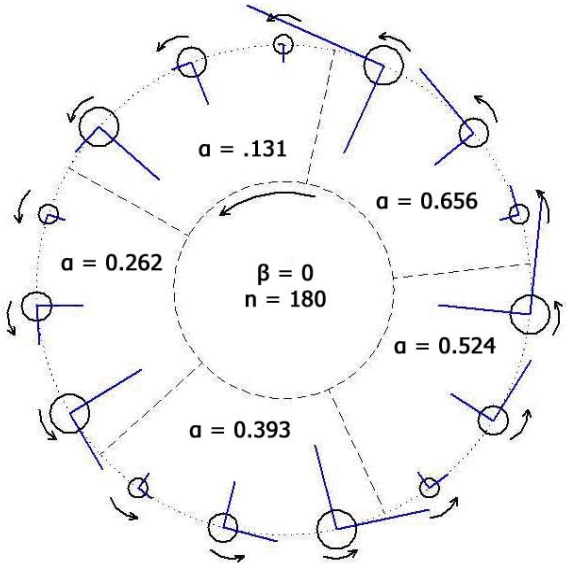

Figure 14. Results for β=0, n=180 and various γ and α.

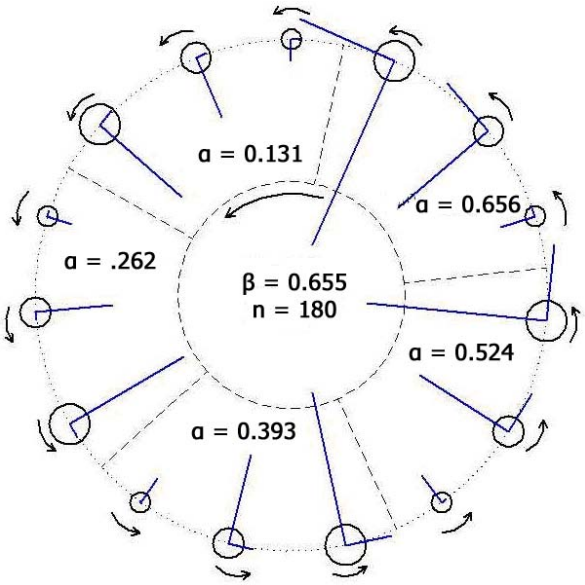

Figure 15. Results for β=0.655, n=180 and various γ and α.

Allowing the cylinders to rotate on the track with β=0.655 produces markedly different results, Fig.15. In particular ratio of tangential to radial component of forces decreases substantially, in some cases(α=0.131,0.262) turning negative, i.e. acting opposite to direction of motion and therefore producing negative work. The combination of the larger γ and larger α produces the best results.

Reducing the number of cylinders by a factor of 2, Fig.16, did not reveal significant changes; only a slight reduction in radial component due to decreased blockage of flow.

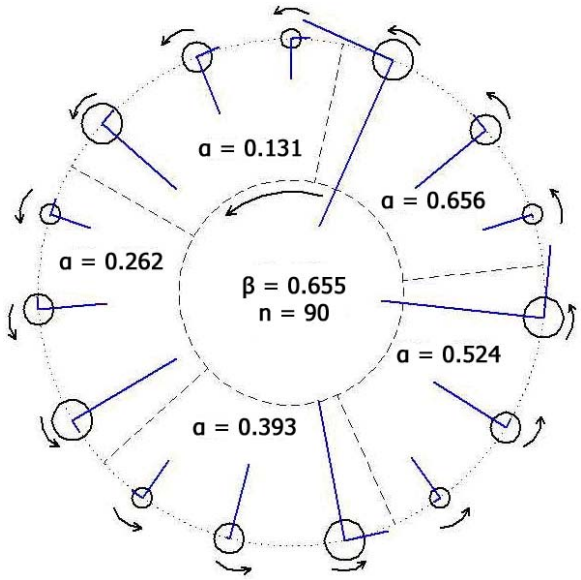

Figure 16. Results for β=0.655, n=90 and various γ and α.

Doubling the value of β to β=1.31 deteriorated the performance considerably, Fig.17. In particular the radial component increased while the tangential component decreased. For values of α smaller than α=0.656 the tangential force component was actually acting opposite to direction of cylinder motion on track; i.e. producing negative work. This indicates that a value of β=1.31 with the current combinations of α and n is far too big.

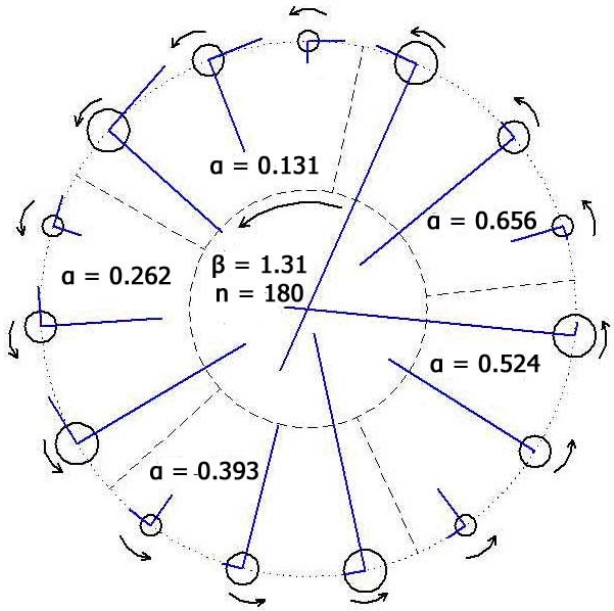

Figure 17. Results for β=1.31, n=180 and various γ and α.

All the previously displayed results were obtained for V=10 m/s; as initially it was assumed that the absolute value of V would have no effect on results, since Reynold's number of the flow is high. However, further investigations revealed this not to be true, as will be shown later.

PERFORMANCE OF MAGNUS-ROTORS

The best description of the performance of the proposed rotor system is the efficiency of converting the kinetic energy of the induced draft into mechanical/electrical power. For the current investigations only the hydraulic efficiency is of concern. The hydraulic efficiency η_h is defined as the ratio of the gross mechanical power output to the power available in the induced draft in absence of the rotors. It is expressed by :

$$\eta_h = \frac{P_M}{\pi R \rho V^3} \tag{1}$$

where P_M is the gross mechanical power output per unit height of rotor, and ρ is air density. It is expressed by the following relation:

$$P_M = n \times (F_T \times \Omega \times R - \omega \int_0^{2\pi} \tau_w . r^2 d\theta) \tag{2}$$

where F_T is the component of the wind force acting on the cylinder tangential to local track direction, and τ_w is the local shear stress at the surface of the cylinder. The mechanical friction losses on the track, in cylinder bearings, and other mechanical linkages are not considered in P_M , hence the "gross" designation.

Figure18 displays the hydraulic efficiency variation with α for various induced draft speeds, for β= 1.0, γ=0.004 and n=180. The latter values where found by relatively crude optimization to yield best performance results. It is noticed that η_h increases with V up to the maximum value of V considered (40 m/s), but improvement asymptotes with further increase of V. Larger values of V are not considered here as they would normally not be achievable in a Solar updraft tower, without use of convergent divergent ducting which is expensive and introduces further hydraulic losses.

Since all other parameters are fixed, the increase of η_h with V is attributed to the solidity ratios employed being too high for the lowest values of V. Thus trailing rotors are affected by the wakes generated by leading ones. This phenomena is well known in wind turbine design(e.g. [11]). The solidity ratio is $(n\gamma)/\pi$, and hence for a given V, improvements in η_h may be brought about by decreasing either n or γ, however this was not investigated.

Figure 18 reveals that the maximum hydraulic efficiency is around 87%, which is close to some hydraulic turbines, although slightly inferior to large-sized Kaplan Turbines.

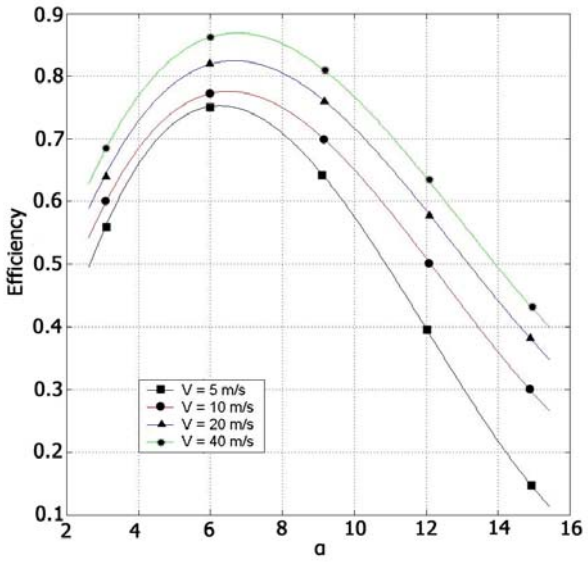

Figure 18. Hydraulic efficiency versus α for various V

SUMMARY & CONCLUSION

The paper proposes the use of Magnus effect rotors instead of conventional axial turbines in Solar updraft towers. An analysis of the flow pattern and resulting forces shows that the performance of the rotors is very sensitive to the proper selection of operational parameters. Using primitive optimization, a hydraulic efficiency of 87% is achieved, which should be improved if more rigorous optimization is employed.

Moreover, the construction of cylinders is considerably cheaper than the manufacture of turbine blades, and therefore even with a slight drop in efficiency it may still make economic sense to go for the Magnus effect rotors. The Magnus rotors also have the superior advantage that they may be manufactured locally employing local expertise in underdeveloped countries, and performance is not expected to deteriorate with time as fast as blades exposed to a harsh environment.

It is thus concluded that the concept is promising and worthy of further investigations.

REFERENCES

[1] Schlaich,J., Bergermann,R., Scheil,W. and Weinrebe,G., 2005, " Design of Commercial Solar Updraft Tower Systems – Utilization of Solar Induced Convective Flows for Power Generation", Solar Energy Engineering, 127, pp.17-24.

[2] Petela,R.,2009, "Thermodynamic Study of a Simplified Model of the Solar Chimney Power Plant"", Solar Energy, 83, pp.94-107.

[3] Ming.,T., Liu,W., Pan,Y. and Xu,G., 2008, "Numerical Analysis of Flow and Heat Transfer Characteristics in Solar Chimney Power Plants with Energy Storage Layer", Energy Conversion and Management, 49, pp. 72-79

[4] Haaf,W., Freidrich,K., Mayr,G. and Schlaich,J. , 1983, "Solar Chimneys, Part I: Principle and Construction of the Pilot Plant in Manzanares", Solar Energy,2, 3-20.

[5] Von Backstrom,T.W., and Gannon,A.J.,2004, "Solar Chimney Turbine Characteristics", Solar Energy, 76.235-41.

[6] Fluri,T.P. and Von Backstrom, T.W. , 2008, "Comparison of Modelling Approaches and Layouts for Solar Chimney Turbines", Solar Energy, 82, pp.239-246.

[7] Denantes,F. and Bilgen,E., 2006, "Counter-rotating Turbines for Solar Cghimney Power Plants", Renewable Energy, 31, pp.1873-1891.

[8] Serag-eldin,M.A., 2005, "Analysis of Effect of geometric Parameters on Performance of Solar Chimney Plants", Proc. ASME 2005 Summer H.T. Conference, San Francisco, paper#2005-72340.

[9]Yakhot,V., Orszag,S., 1986, "Renormalization Group Analysis of Turbulence. I. Basic Theory", J. Scientific Computing ,1,pp.3-51.

[10] Launder,B.E. and Spalding,D.B. , 1974, " The Numerical Computation of Turbulent Flows", J. Computer Methods in Applied Mechanics and Eng., 3, pp269-289.

[11] Twidell,J. and Weir,T., 2006, "Renewable Energy Resources", 2nd edition, Taylor & Francis, London and NY, Chapter 9.

